

Methods

Synthesis of $\text{NH}_4\text{V}_4\text{O}_{10}$. Ammonium vanadate was synthesized by hydrothermal method. 2.74 mmol of NH_4VO_3 powers (Aladdin, $\geq 99\%$) and 4.6 mmol of $\text{C}_2\text{H}_2\text{O}_4 \cdot 2\text{H}_2\text{O}$ powers (Macklin, $\geq 99.5\%$) were dispersed in 40.0 mL deionized water first, and then the yellow-greenish solution was obtained after magnetic stirring for 30 min at room temperature. The mixed solution was putted into the reaction kettle to heat at 180 °C for 3 h. After cooling to room temperature, the product was obtained by washing with deionized water and anhydrous ethanol for few times. The $\text{NH}_4\text{V}_4\text{O}_{10}$ was obtained after drying in a vacuum drying box at 60 °C for 24 hours.

Synthesis of $\text{NH}_4\text{V}_4\text{O}_{10}$ cathode. The synthetic $\text{NH}_4\text{V}_4\text{O}_{10}$ powder active material (70 wt%), carbon black (20 wt%) and polyvinylidene fluoride (PVDF) (10 wt%) in N-Methyl pyrrolidone solvent. The mixture powders were ground with a pestle for 30 min. Homogeneous slurries were obtained, and the slurries were uniformly pasted onto high purity titanium foil and dried in a vacuum drying oven at 60 °C for 12 h. Ti foil with a thickness of 0.005 mm was used as current collector.

Electrochemical Tests. The preparation of electrolytes was carried out by mixing GN (Aladdin, $>96.0\%$) and $\text{Zn}(\text{ClO}_4)_2 \cdot 6\text{H}_2\text{O}$ (Aladdin) with molarity of 0.5, 1.0, 1.5, and 2.0 at room temperature and then stirring until clear solutions were obtained. Galvanostatic charge/discharge tests of all coin cells were measured on LAND CT2001A test system. Coin cells (2032 type) were assembled by fiberglass diaphragm and electrode pieces. Fiberglass diaphragm soaked with electrolytes was placed in between the prepared cathode and Zn anodes in an open atmosphere. Each cell contains 130 μL electrolytes. The reversibility and cycle stability of $\text{NH}_4\text{V}_4\text{O}_{10}$ cathodes of the full cells were tested with the voltage window from 0.4 to 1.6 V. Cyclic voltametric (CV) and electrochemical impedance spectroscopy (EIS) were carried out on Metrohm (PGSTAT302N) Autolab electrochemical workstation. Among them, the Zn/Ti cells were tested by cyclic voltammetry at a scanning rate of 2 mVs^{-1} within the voltage range from -0.2 to 2.0 V. To test the voltage window of the battery, a large voltage range from -0.3 to 2.5 V was conducted.

Materials characterizations. The phase and structure of the samples were characterized by power X-ray diffractometer (XRD, Cu-K α , $\lambda=1.5405 \text{ \AA}$). Morphologies of samples were observed by scanning electron microscope (SEM, JEOL, JSM-6700F) and transmission electron microscope (TEM, FEI TITAN THEMIS 200). The Raman spectra was recorded by using Thermo Scientific DXRXI system with excitation from an Ar laser at 532 nm. The element valence and chemical valence samples were determined by X-ray photoelectron spectroscopy (XPS, Nexsa, ThermoFisher) on PHI5300 instrument, and cycled Zn plates were washed by deionized water before XRD, XPS and SEM tests.

MD simulations. MD simulations were conducted using Forcite code of Material Studio software. In the MD simulations process, the electrolyte molecules with the molar ratios of GN, Zn(ClO₄)₂, and H₂O for 6.6:1:6 were packed in a simulation box. The simulations were performed using COMPASSII force field, a time step of 1 fs, a simulation time of 10 ns, and the canonical ensemble NVT at 303K. The mean square displacement (MSD) and radial distribution function (RDF) were obtained based on the MD simulations. Density Functional Theory (DFT) based quantum chemical calculations were conducted using the Dmol3 module. The interatomic distance was obtained by geometry optimization with the m-GGA and M06-L. The binding energy of $\Delta E(\text{Zn}^{2+}\text{-H}_2\text{O})$ and $\Delta E(\text{Zn}^{2+}\text{-GN})$ was calculated according to the Equation as following:

$$\Delta E(\text{Zn}^{2+}\text{-H}_2\text{O}) = E_{\text{total}} - E(\text{Zn}^{2+}) - E(\text{H}_2\text{O})$$

$$\Delta E(\text{Zn}^{2+}\text{-GN}) = E_{\text{total}} - E(\text{Zn}^{2+}) - E(\text{GN})$$

where E_{total} is the structure total energy.

ZGN

ZHO

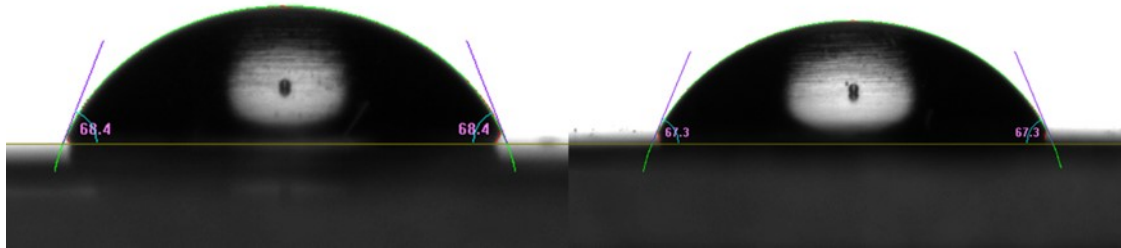


Figure S1. Contact angle of the ZGN and ZHO electrolytes on Zn anode.

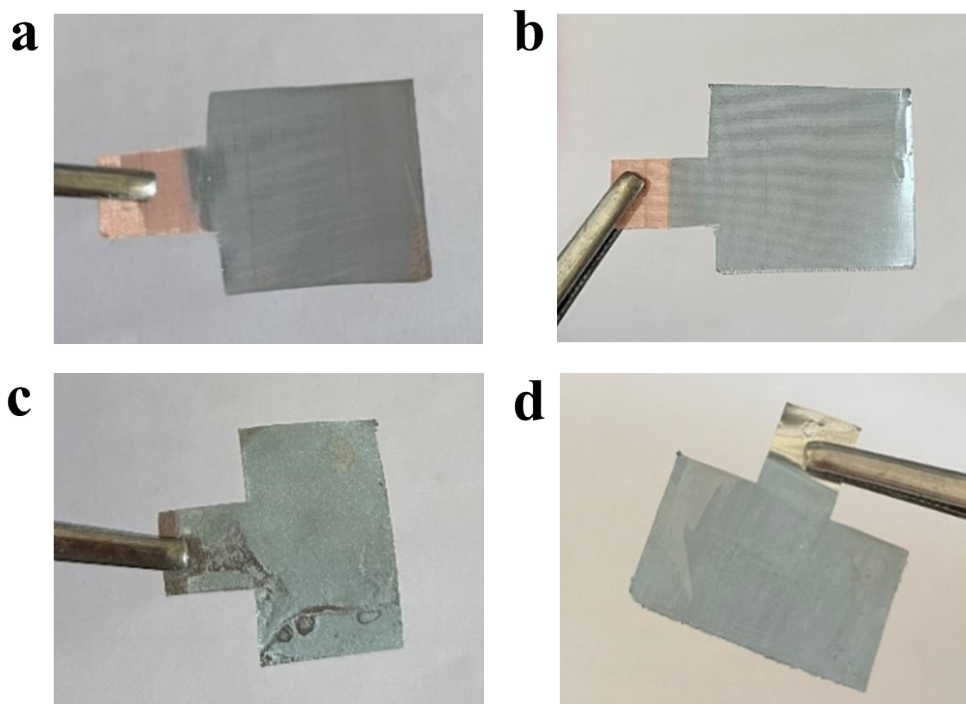


Figure S2. Optical images of Zn plated in (a) ZHO and (b) ZGN on the copper mesh, in (c) ZHO and (d) ZGN on the Zn foil.

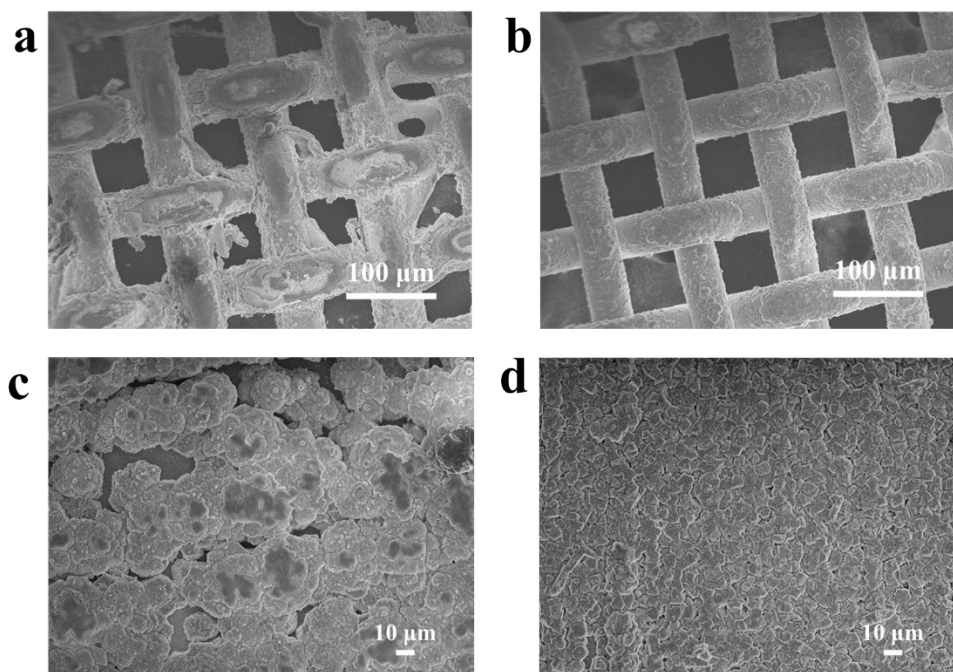


Figure S3. SEM images of Zn plated in (a) ZHO and (b) ZGN on the copper mesh, in (c) ZHO and (d) ZGN on the Zn foil.

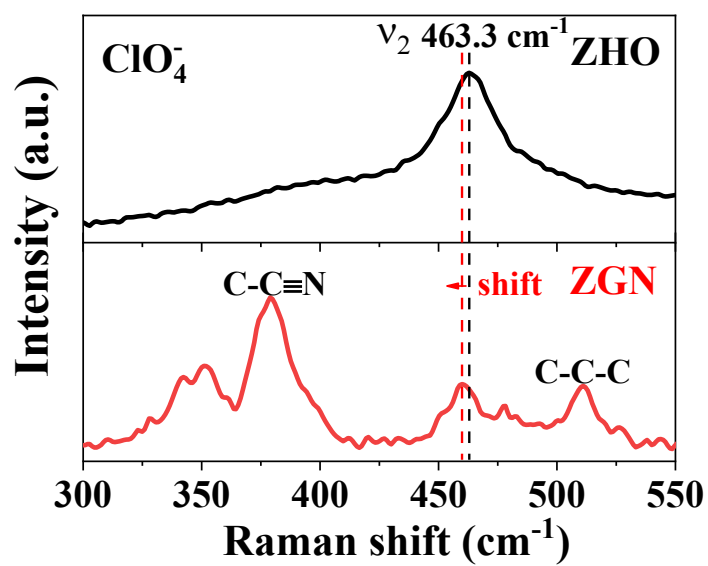


Figure S4. Raman spectra of ν_2 mode of ClO_4^- in ZHO and ZGN.

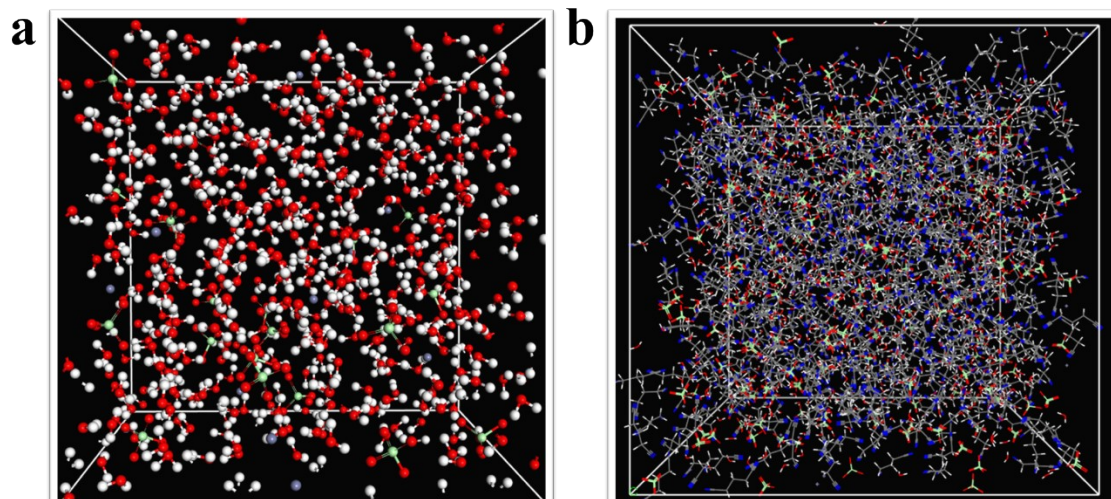


Figure S5. 3D snapshots obtained by MD simulations in (a) ZHO and (b) ZGN.

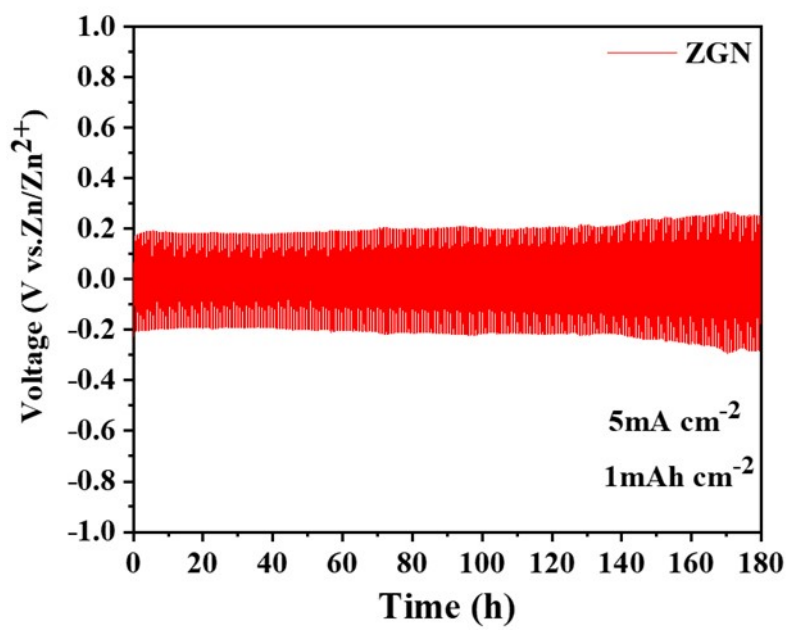


Figure S6. The voltage curve of Zn||Zn cell at 5.0 mA cm^{-2} for 1.0 mAh cm^{-2} .

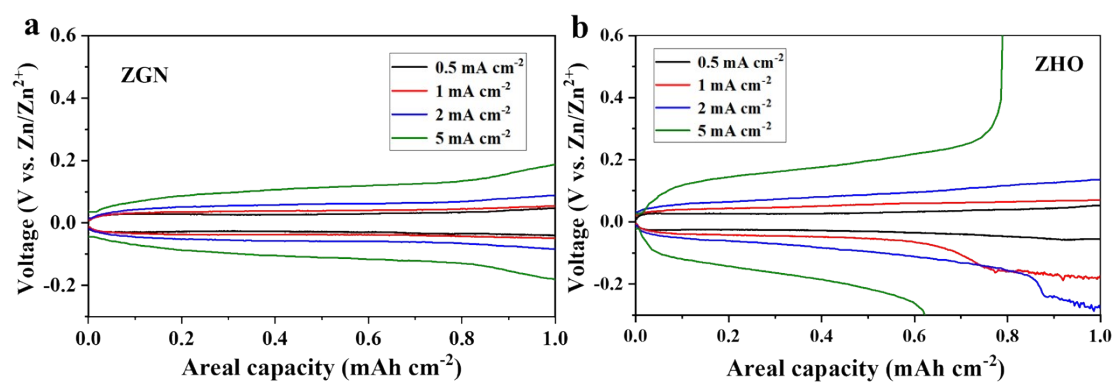


Figure S7. The corresponding voltage profiles of the Zn||Zn cells at current densities from 0.5 to 5 mA cm⁻² with the specific capacity of 0.5 mAh cm⁻² in (a) ZGN and (b) ZHO.

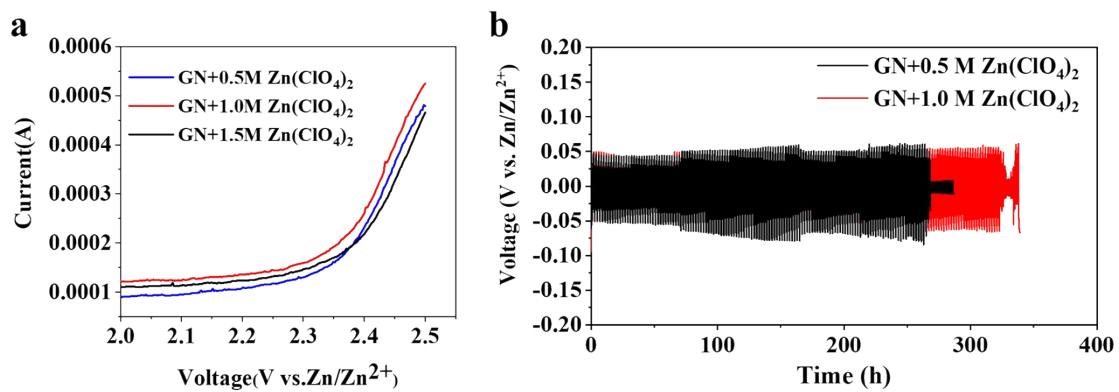


Figure S8. The electrochemical windows of Zn||Ti cells (a) and the voltage curves of Zn||Zn cells (b) with different concentration of Zn salt.



Figure S9. Photograph of the disassembled Zn/Zn cells after cycling in ZHO.



Figure S10. Photograph of the disassembled Zn/Zn cells after cycling in ZGN.

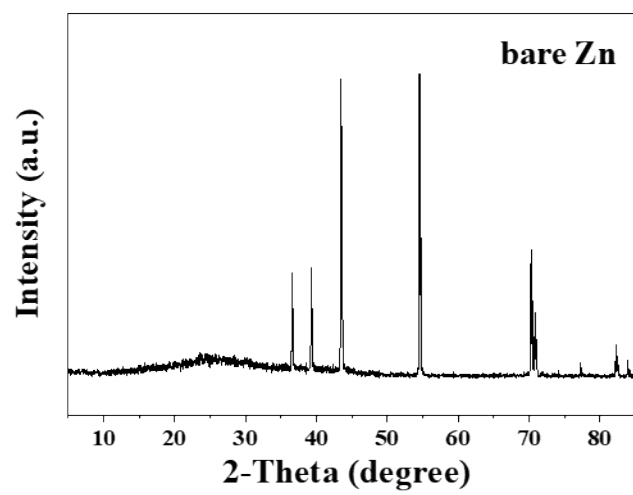


Figure S11. XRD pattern of bare Zn.

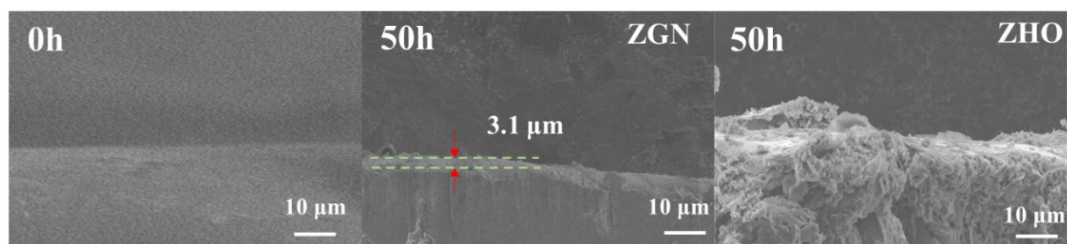
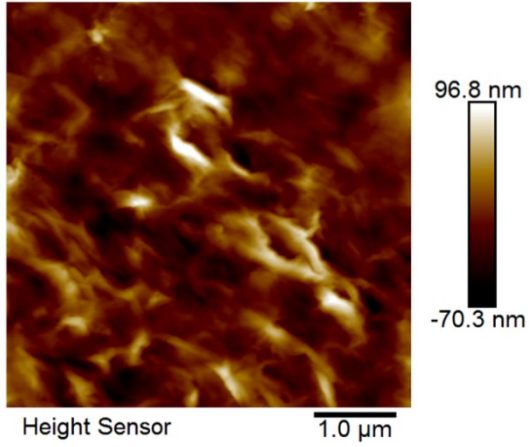


Figure S12. SEM images of the Zn electrode after cycled for 50h in the Zn||Zn cells with different electrolytes.

ZGN



ZHO

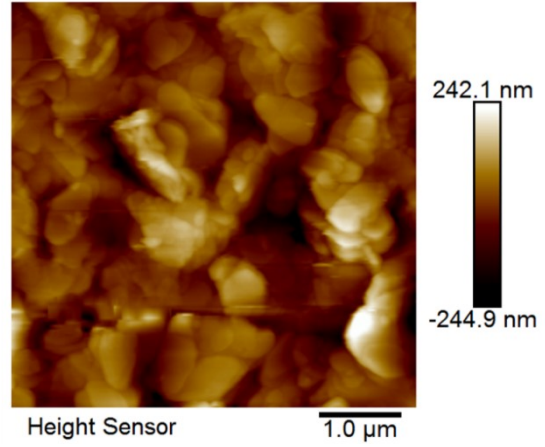


Figure S13. AFM images of the Zn electrode after cycled for 50h in the Zn||Zn cells with different electrolytes.

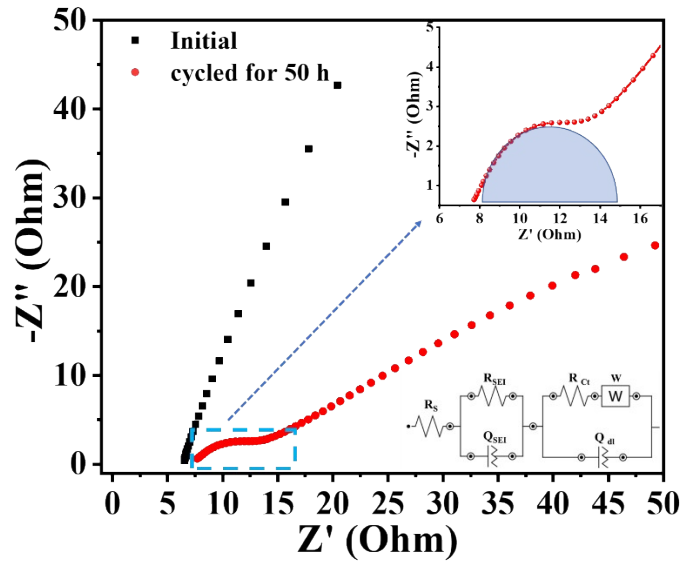


Figure S14. Fitted EIS spectra of the Zn||Zn symmetrical cells. The upper inset is an enlargement of the indicated range, and the lower inset is the equivalent circuit. The ionic conductivity of SEI can be estimated based on the following equation:

$$\sigma = \frac{L}{S \cdot R_b}$$

where R_b is the bulk resistance obtained by EIS measurements (7.7Ω in this work), S is the area (1.13 cm^2 in this work), and L is the thickness of the SEI layer ($3.1 \mu\text{m}$ in this work). Therefore, the ionic conductivity of SEI is evaluated as $\sigma = 3.6 \times 10^{-5} \text{ S cm}^{-1}$.

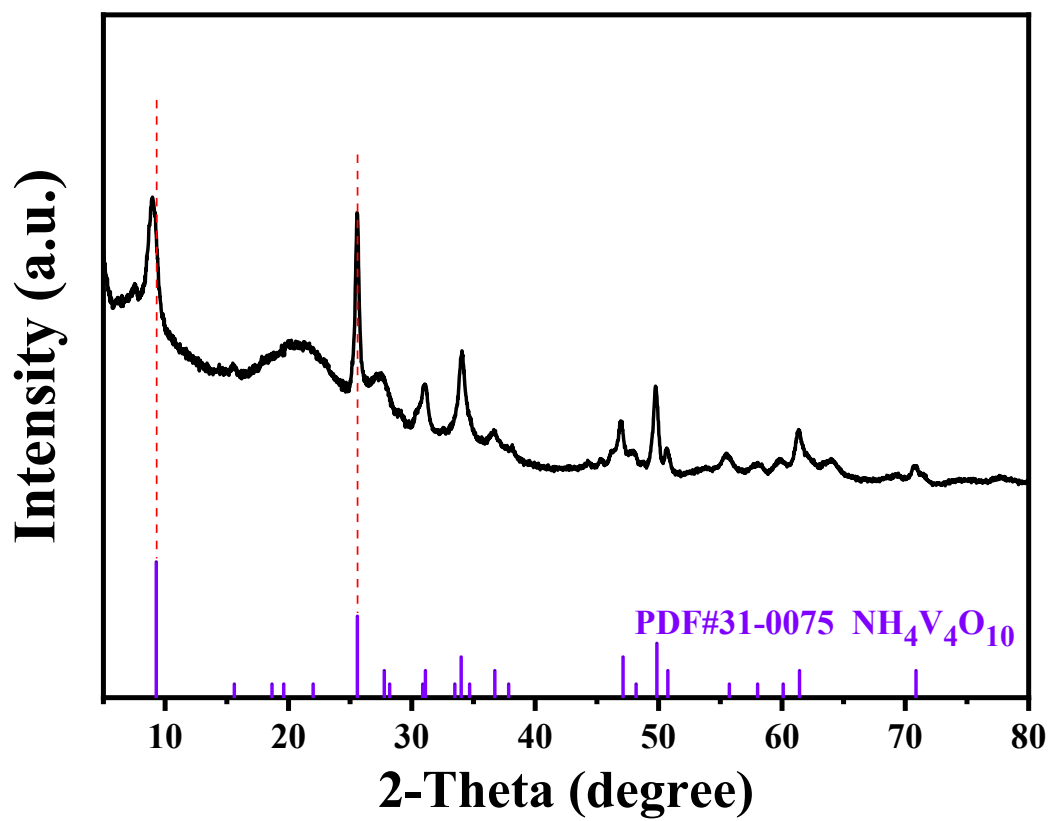


Figure S15. XRD patterns of as-prepared $\text{NH}_4\text{V}_4\text{O}_{10}$.

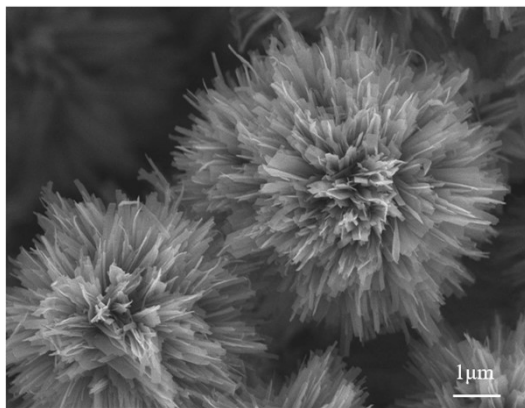


Figure S16. SEM image of as-prepared $\text{NH}_4\text{V}_4\text{O}_{10}$.

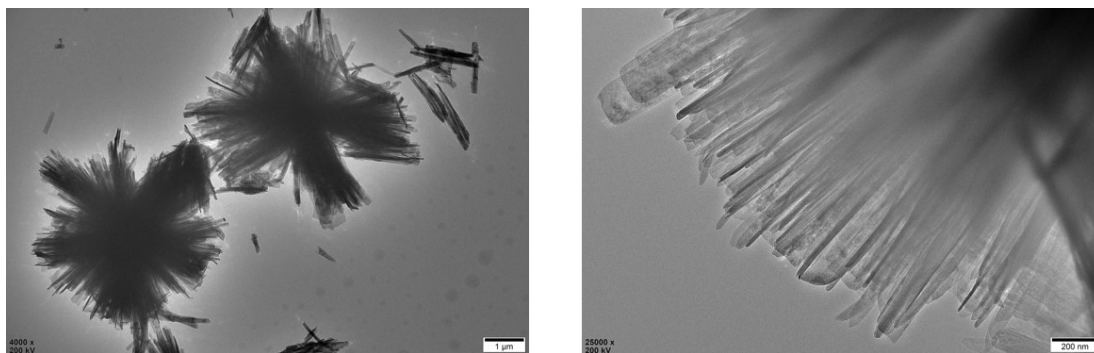


Figure S17. TEM images of as-prepared $\text{NH}_4\text{V}_4\text{O}_{10}$.

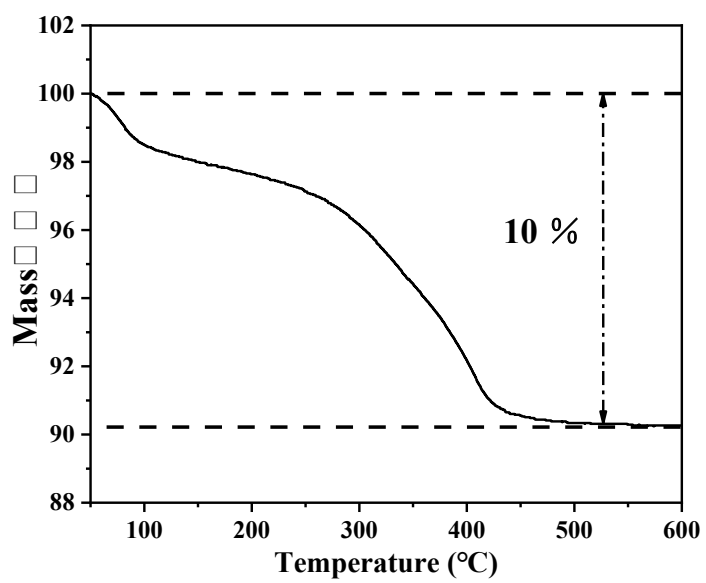


Figure S18. TGA curve of NH₄V₄O₁₀ cathode.

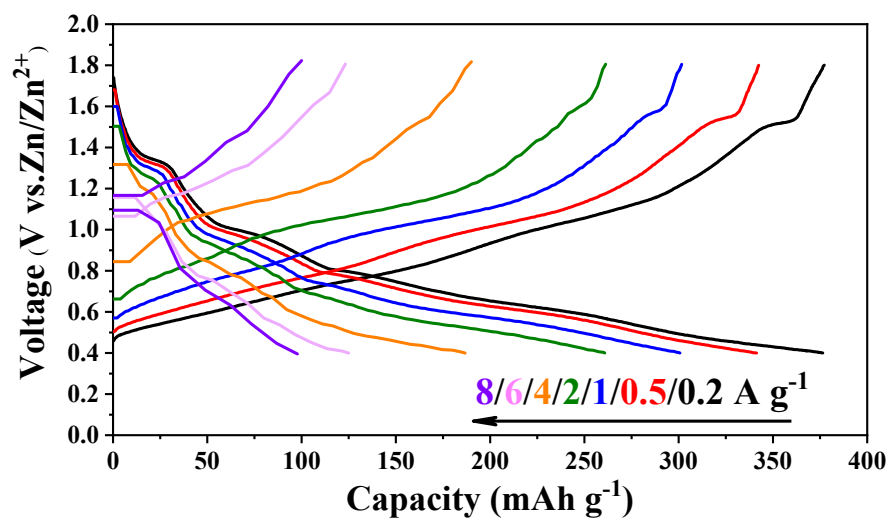
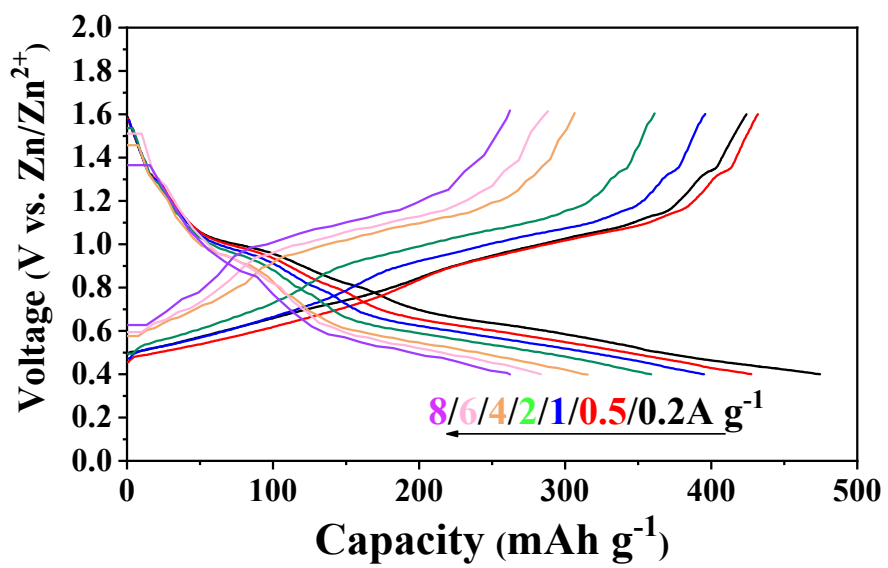


Figure S19. Corresponding discharge/charge profiles of full cells under different current conditions in ZGN.



Fi

Figure S20. Corresponding discharge/charge profiles of full cells under different current conditions in ZHO.

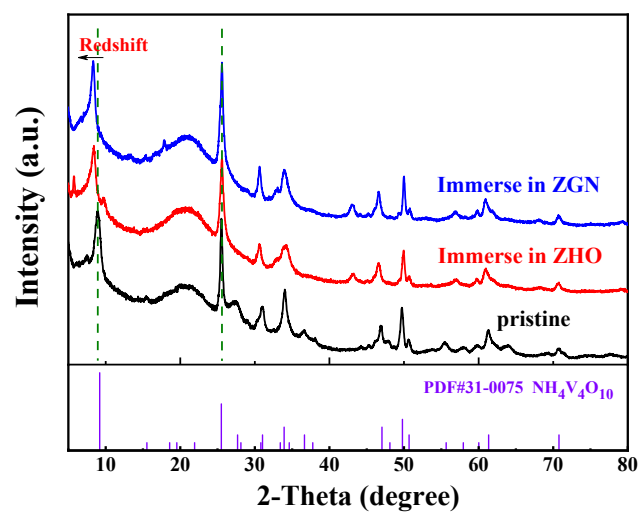


Figure S21. XRD of $\text{NH}_4\text{V}_4\text{O}_{10} \cdot m\text{H}_2\text{O}$ electrode immersed in the ZHO and ZGN electrolytes.



Figure S22. PH value of the ZHO and ZGN electrolytes.

Table S1. The DFT calculations of theoretical binding energy.

	E_{total} (Ha)	ΔE (Ha)	ΔE (eV)
Zn ²⁺ -H ₂ O	-1854.9813033	-0.1442573	-3.9255296476
Zn ²⁺ -GN	-2042.9629921	-0.3354111	-9.1272068532